Scripta Materialia 135 (2017) 63–67

Contents lists available at ScienceDirect

Scripta Materialia

journal homepage: www.elsevier.com/locate/scriptamat

Regular article

Improving the tensile ductility of metal matrix composites by laminated structure: A coupled X-ray tomography and digital image correlation study

Guohua Fan [a,*], Lin Geng [a], Hao Wu [b,*], Kesong Miao [a], Xiping Cui [a], Huijun Kang [c], Tongmin Wang [c], Honglan Xie [d], Tiqiao Xiao [d]

[a] School of Materials Science and Engineering, Harbin Institute of Technology, Harbin 150001, PR China
[b] School of Materials Science and Engineering, University of Jinan, Jinan 250022, PR China
[c] School of Materials Science and Engineering, Dalian University of Technology, Dalian 116000, PR China
[d] Shanghai Synchrotron Radiation Facility, Shanghai 201204, PR China

ARTICLE INFO

Article history:
Received 14 March 2017
Accepted 24 March 2017
Available online xxxx

Keywords:
Metal matrix composites (MMC)
Layered structures
Interfaces
Image analysis
Strain evolution

ABSTRACT

The microstructure design strategy of laminated structure was applied to improve the mechanical properties of metal matrix composites (MMCs). The laminated composites were prepared by hot pressing and rolling of alternately stacked Ti foils and SiC_p/Al composite foils, and exhibited a superior strength-ductility synergy compared to SiC_p/Al bulk MMCs. Coupling X-ray tomography and digital image correlation (DIC) revealed that the enhanced mechanical properties originated from the contribution of the interface on local stress/strain transfer behaviors, thus delaying the crack initiation and propagation within SiC_p/Al layers.

The addition of reinforcements makes metals strong but brittle. The well-known strength-ductility trade-off dilemma of metal matrix composites (MMCs) originates from (i) the easy crack initiation caused by the deformation incompatibility between the matrix and the reinforcements, and (ii) the weak resistance to crack propagation [1,2]. Therefore, how to suppress the crack initiation and propagation of MMCs is a key route to improve their mechanical properties, in particular for the tensile ductility; in essence, the scientific problem is how to artificially control the strain distribution by microstructure design [3–5]. Recent investigations have demonstrated that laminated structure can effectively inhibit the strain localization during the plastic deformation, thus exhibiting a superior strength-ductility combination [6–8]. However, the vast majority of research work focus on the metal-metal laminated composites [9,10]. The potential of MMCs serving as one of laminated components, as well as whether the strategy of laminated structure can be applied in improving the mechanical properties of MMCs or not, remains unclear.

In the past few years, the understanding of strain localization mainly depends on the post-mortem examination of deformed microstructures [11,12], lacking direct visualization of strain evolution process. For this purpose, the technologies of digital image correlation (DIC) and X-ray tomography were recently developed [10,13]. However, both technologies are primarily applied in bulk homogeneous materials [1,2], marginally in the laminated composites. Additionally, coupling DIC and X-ray tomography is very useful to correlate the deformation and fracture behaviors of the composite, but the application of the coupled technology is rarely reported.

In this work, the classical SiC_p/Al composite was selected as referenced MMCs. The microstructure design strategy of laminated structure was used to improve the mechanical properties of SiC_p/Al MMCs. The laminated composite was fabricated by hot pressing and rolling of alternately stacked Ti foils and SiC_p/Al composite foils, and room temperature tensile tests were performed to compare the mechanical properties of SiC_p/Al, Ti, and Ti-(SiC_p/Al) laminated composites. The deformation and fracture behaviors of laminated composites were characterized by coupling DIC and X-ray tomography, and the mechanisms behind the enhanced mechanical properties of laminated composites were elucidated.

Commercially pure Ti foils and in-house fabricated 10 vol% SiC_p/Al composite foils were cut into several rectangles with dimensions of 30 mm width by 50 mm length, chemically etched to a final thickness of 160 μm and 150 μm, respectively, alternately stacked, and then hot pressed at 515 °C under 75 MPa for 1.5 h, followed by hot rolling through 6 passes to a total thickness reduction of 30%. The rolling temperature was selected as 500 °C, and before every rolling pass, the

* Corresponding authors.
E-mail addresses: ghfan@hit.edu.cn (G. Fan), mse_wuh@ujn.edu.cn (H. Wu).

http://dx.doi.org/10.1016/j.scriptamat.2017.03.030
1359-6462/

sample was annealed at 500 °C for 10 min. The details of sample preparation can be referred to our previous work [10].

An Olympus optical microscope (OM), and a FEI Tecnai F30 transmission electron microscope (TEM) were employed for microstructure observation. The mechanical properties of laminated composites and SiC_p/Al bulk MMCs were evaluated by room temperature tensile tests. The gauge dimensions of tensile specimens were 5 mm width by 18 mm length by 2 mm thickness, and the tensile tests were performed using an Instron-1186 universal testing machine at a strain rate of $1 \times 10^{-4}\,s^{-1}$. The tensile fractured specimen was then examined by X-ray tomography (Shanghai Synchrotron Radiation Facility, SSRF) for direct visualization of the spatial distribution of cracks [13]. The X-ray beam energy was 28 keV, and the spatial resolution of X-ray tomography was 0.65 μm. The VGStudioMax software was used for data post-processing.

The laminated composite was deformed with in situ OM imaging (the latter provided a large field-of-view with representative statistics). The deformation was carried out by uniaxial tensile loading to different strain levels at a displacement rate of 2 μm/s through a screw-driven Kammrath & Weiss GmbH tensile stage (Dortmund, Germany), and the specimen geometries were 2 mm thickness by 2 mm width by 18 mm length. A commercial VIC-2D software was utilized for DIC analysis and the calculation of local strain fields.

The laminated composites, composed of alternating layers of Ti and SiC_p/Al as shown in the inset of Fig. 1b, were successfully prepared in the present work, and the thicknesses of both components were measured as 110 ± 10 μm (Ti layers) and 100 ± 9 μm (SiC_p/Al layers), respectively. In between both layers, there exists a 25 nm-thickness $TiAl_3$ layer (Supplementary Fig. S1), probably due to the process of hot pressing and rolling during the sample preparation. Despite the presence of nano-sized $TiAl_3$ layers, the mechanical properties of laminated composites were still higher than those of SiC_p/Al bulk MMCs (Fig. 1a and Table 1). Additionally, the volume fraction of SiC_p also plays a very important role on the mechanical properties of Ti-(SiC_p/Al) laminated composites as shown in Fig. 1b and Table 1.

Taking 10 vol% SiC_p/Al bulk MMCs for example, the ultimate tensile strength of Ti-(10 vol.% SiC_p/Al) laminated composite increased up to 363 MPa, while the elongation of laminated composite is double that of bulk MMCs (Table 1). In order to explain the underlying mechanism of such improved mechanical properties, we firstly compared the three-dimensional fracture characteristics of both samples, and several of important results were summarized as follows: (i) The large flake-like cracks in SiC_p/Al MMCs (Fig. 2c) were in sharp contrast to many small cracks with globular morphology in laminated composites (Fig. 2a), and the latter was more clearly observed in reconstructed slices as shown in Supplementary Fig. S3. (ii) In the case of bulk MMCs, the plastic deformation was highly localized [2]. For example, the reduction of area in 20 vol% SiC_p/6061Al was only 3% nearby the fracture surface, and almost zero at 5 mm-away from the fracture surface [14]. However, a wide crack distribution was observed in laminated composites (Fig. 2b), indicative of a more homogeneous deformation mode and implying that the grains far away from the fracture surface sufficiently participated into the plastic deformation [7,11]. (iii) No crack was found in the Ti layers of laminated composites, and the laminated composite was fractured by SiC_p/Al cracking and interfacial decohesion (Fig. 2d and Supplementary Fig. S3). The fundamental mechanism behind the observed interfacial delamination will be discussed later. Additionally, it seems plausible from Supplementary Fig. S3 that the presence of Ti layers restricted the crack propagation behavior within the SiC_p/Al layers, and that cracks penetrating into the Ti layers were strictly inhibited.

Table 1
Mechanical properties of SiC_p/Al, Ti, and laminated composites.

Material systems	Ultimate tensile strength (MPa)	Elongation (%)
10 vol.% SiC_p/Al MMCs	156 ± 11	11.8 ± 1.2
As-rolled Ti	571 ± 29	21.6 ± 1.7
Ti-(0 vol.% SiC_p/Al) laminates	276 ± 18	34.5 ± 2.3
Ti-(3 vol.% SiC_p/Al) laminates	341 ± 22	31.4 ± 2.1
Ti-(5 vol.% SiC_p/Al) laminates	351 ± 23	30.6 ± 1.8
Ti-(10 vol.% SiC_p/Al) laminates	363 ± 25	24.5 ± 1.5

Fig. 3 shows real-time visualization of strain evolution process of laminated composites during the tensile deformation. The strain tensor component used for DIC analysis was selected as *xx* normal strain (ε_{xx}, along the horizontal direction). The region of interest (ROI) was labeled by black dotted ellipse, which vividly describes how localized strains within SiC_p/Al layers transferred into the neighboring Ti layers, and finally back to the SiC_p/Al layers with increasing tensile strains (Fig. 3). This "reversed" strain transfer path seems impossible for SiC_p/Al MMCs (Supplementary Fig. S4) or as-rolled Ti (Supplementary Fig. S5), and also indicates the stress partitioning nearby the interface between SiC_p/Al layers and Ti layers [12,15]. At the same time, the positive ε_{xx} strain at the ROI was gradually changed to the negative ε_{xx} strain when the macroscopically true strains increased from 0.3% to 4.0% (Supplementary movie 1). Additionally, the contribution of the interface on local stress/strain transfer was intuitively apparent: (i) As the tensile deformation progressed, several of regions in SiC_p/Al layers nearby the ROI, with a local strain level of nearly zero at the early deformation stage, started to participate into the plastic deformation, and the loads were not transmitted by themselves, but by the interface and the shear stress that the adjacent Ti layer exerted [15,16]; (ii) Deformation was no longer localized within the SiC_p/Al layers, and strong strain transfer effect was observed, which may reduce the local stress concentration of SiC_p/Al layers and effectively suppress the crack initiation and propagation within SiC_p/Al layers [17]; (iii) The localized deformation, especially along crystallographic ⟨*c*⟩ direction, of as-rolled Ti (caused by strong basal texture, Supplementary Fig. S2) was stabilized by laminated structure, thus leading to a larger tensile ductility as shown in Fig. 1a.

Quantitative measurements of ε_{xx} strain tensor component as a function of tensile strains indicate the change in deformation mechanisms of

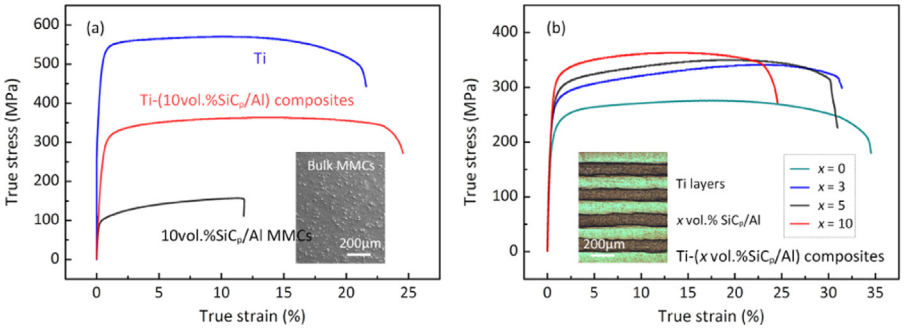

Fig. 1. Tensile stress-strain curves of (a) bulk MMCs, Ti, and laminated composites with the same processing route, and (b) Ti-(*x*vol.% SiC_p/Al) laminated composites ($x = 0, 3, 5, 10$).

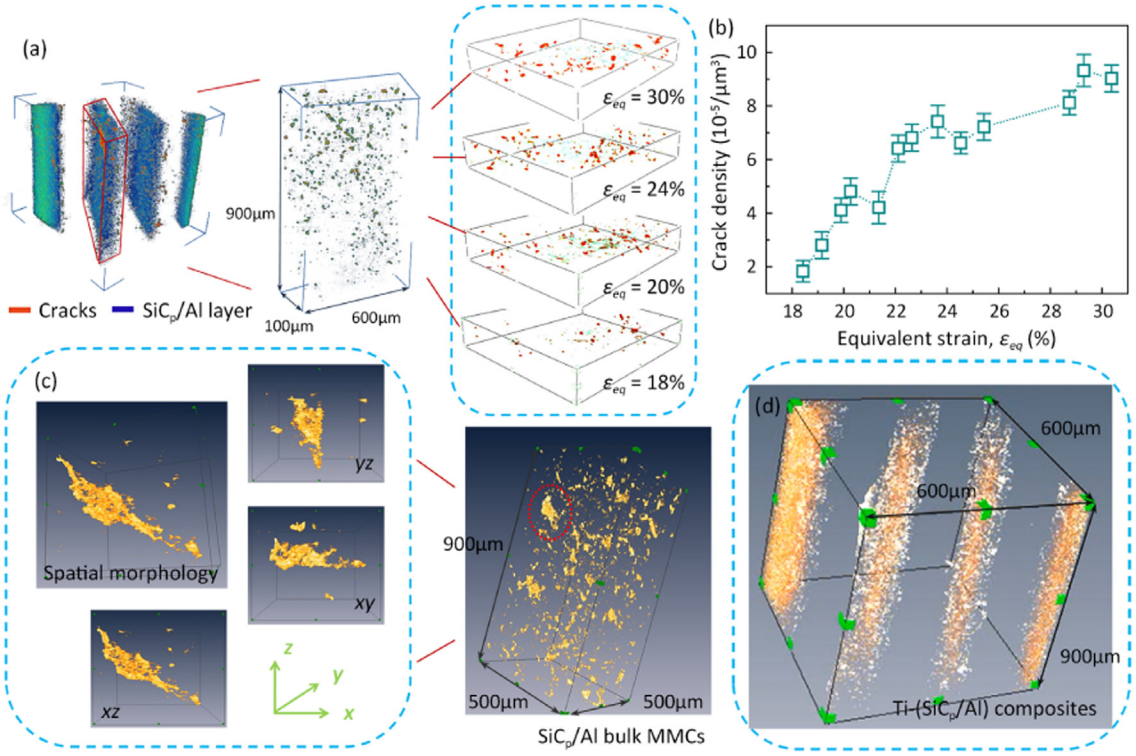

Fig. 2. Three-dimensional characterizations of fracture surfaces of (a), (b), and (d) Ti-(10 vol.% SiC_p/Al) laminated composites, and (c) 10 vol.% SiC_p/Al bulk MMCs. The definition of equivalent strain, ε_{eq}, was introduction to represent the local strain levels, and determined by $\varepsilon_{eq} = \ln(S_0 / S)$ [11], where S_0 and S denote the section area for unstrained samples and the area of cross-section at a certain position, respectively. In (a), (c) and (d), the equivalent strain levels gradually increased from bottom to top, and the voxels corresponding to the matrix were omitted to facilitate the visualization of crack distribution.

laminated composites (Fig. 4). The critical transition point is a strain at which interfacial delamination occurred. When the macroscopically true strain was below 6%, an isostrain condition was strongly suggested [15], during which the well-bonded interface sufficiently exerted the stress/strain transfer capability (Fig. 3 and Supplementary movie 1). It should be mentioned here that the difference in the ε_{xx} strain levels of

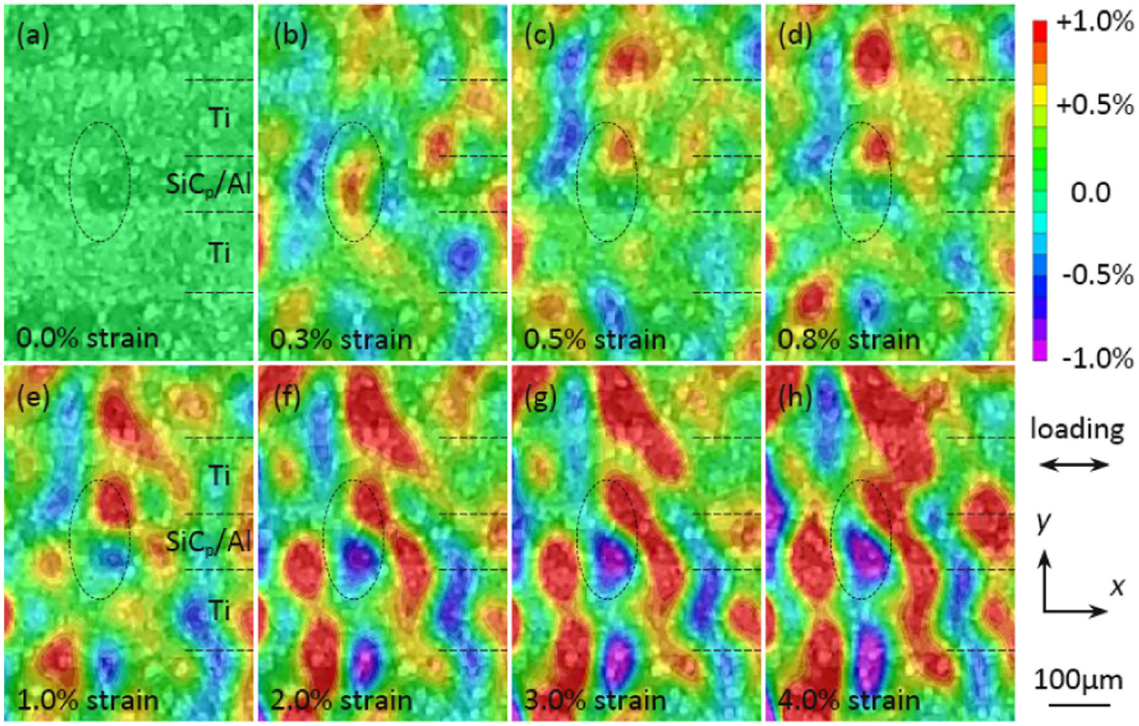

Fig. 3. Evolution of the horizontal strain tensor (ε_{xx}) during the tensile deformation. The Ti layers and SiC_p/Al layers are both schematically highlighted by black dotted lines. The macroscopically true strains, at which we captured the OM images, are labeled at the bottom left corner of each snapshot.

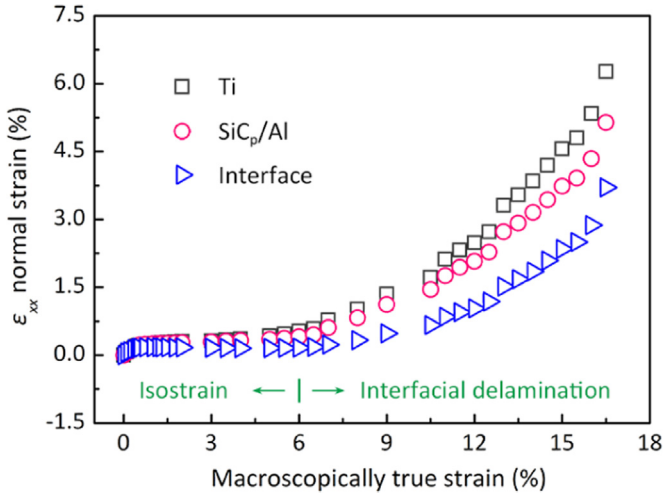

Fig. 4. Quantitative measurements of ε_{xx} strain tensor with increasing true strains.

Ti layers, SiC_p/Al layers, and the interface was progressively growing with increasing true strains, in particular at strains of more than 6%, implying the local interfacial delamination may take place [10]. This inference was rationalized by the dynamic evolution process of shear strains (Supplementary Fig. S6), where a pair of shear strains with opposite signs were clearly observed nearby the interface between Ti layers and SiC_p/Al layers when the macroscopically tensile strain increased up to ~6.0%, which may "tear" the interface and result in the local interfacial delamination (Supplementary Fig. S3).

There are many reasons that account for the occurrence of interfacial delamination: (i) Firstly, deformation incompatibility between Ti layers and SiC_p/Al layers may produce the strain gradient near the interface (Fig. 3), which needs to be accommodated by the generation of geometrically necessary dislocations [4,6,18]. (ii) It is widely accepted that the slip transmission is favored geometrically when the slip systems on both sides of the interface are parallel to each other [9]. However in the present work, neither orientation relationship nor parallel slip plane was found at the Ti/$TiAl_3$ and Al/$TiAl_3$ interface (Supplementary Fig. S1). Under such an interfacial condition, dislocations gliding on either Ti layers or SiC_p/Al layers were severely confined by the interface, and then spontaneously deposited at the interfaces. (iii) A nano-sized $TiAl_3$ layer was formed at the interface between Ti layers and SiC_p/Al layers during the sample preparation process (Supplementary Fig. S1). Although the size effect can influence the mechanical properties of $TiAl_3$ layers [19], their intrinsic brittleness may be not fundamentally changed. Therefore, the brittle $TiAl_3$ layer and a high dislocation density at the interface synergistically induce the interfacial delamination at strains of more than 6%.

It is concluded from Fig. 1a that the SiC_p/Al layer is the soft component in the Ti-(10 vol.% SiC_p/Al) laminated composites despite the addition of 10 vol% SiC_p reinforcements. Recent micromechanics investigations of brittle/ductile multilayered composites and gradient-structured materials have demonstrated that (i) the soft component, for example, the SiC_p/Al layer in the current work, yields first, while the hard component of the Ti layer still elastically deforms [3]; and that (ii) the laminated composites or gradient-structured materials may be fractured when the hardness or nanohardness of soft component (SiC_p/Al) increased up to the same order of magnitude compared to that of hard component [8,12]. In other words, laminated structure prolonged the work hardening of SiC_p/Al layers to larger plastic strains [6,18,20], so that they can plastically deform in a more stable manner compared to SiC_p/Al bulk MMCs. This inference is also experimentally supported by the sharp drop for bulk MMCs and the slow decrease for laminated composites at the end part of both tensile curves (Fig. 1), and the latter implies that laminated composites exhibit a good resistance to crack propagation and an enhanced tensile stability [7].

Generally, either the SiC_p cracking or SiC_p-Al interfacial decohesion is the predominant fracture mechanism of SiC_p/Al bulk MMCs [1], and the addition of SiC_p reinforcement seriously worsens the tensile ductility of SiC_p/Al MMCs. An extreme case is that the 20 vol% SiC_p/Al MMCs may break in a brittle manner, which is caused by high strain localization (the high dislocation density of deformed microstructure is limited to a very narrow region) [14]. However when the plastic deformation of the SiC_p/Al layer was confined by neighboring Ti layers, a significant improvement in tensile ductility was observed in Fig. 1. Combining X-ray tomography and in situ DIC revealed that the enhanced ductility originated from the contribution of the interface on local stress/strain transfer behavior. A direct evidence was the experimentally observed local strain transfer from SiC_p/Al layers to adjacent Ti layers (Fig. 3). As a result, the stress concentration of SiC_p/Al layers during the tensile deformation was largely decreased, thus effectively delaying the crack initiation and propagation within SiC_p/Al layers, and also explaining the formation of small cracks with sizes of less than 10 μm at an equivalent strain of 13.4% (Supplementary Fig. S3). Also, several of highly deformed regions in SiC_p/Al layers, that ought to be fractured, may recover the potential of further plastic deformation due to the local stress/strain transfer effect (Fig. 3), and therefore laminated composites could continue to deform plastically even if the macroscopically applied strain was far more than the tensile ductility of SiC_p/Al layers [15].

Before closing the paper, it should be mentioned that the presence of $TiAl_3$ layers may influence the effect of the interface on the local stress/strain transfer, which is detrimental to the mechanical properties. The future work will focus on suppressing the formation of interfacial phases by selecting appropriate processing parameters or other binary material systems.

In summary, the Ti-(SiC_p/Al) laminated composite was fabricated in the present work, and significant improvements in the mechanical properties were found compared to SiC_p/Al bulk MMCs. Coupling X-ray tomography and in situ DIC revealed that the enhanced mechanical properties resulted from the contribution of the interface on local stress/strain transfer behaviors, so that the crack initiation and propagation of SiC_p/Al layers were strongly suppressed. Our work also suggested that the mechanical properties of laminated composites can be further improved by controlling the formation of interfacial phases.

This work was financially supported by the National Natural Science Foundation of China (Grant No. 51571070, 51571071). H. Wu would like to acknowledge the project supported by the Science Foundation from the University of Jinan (Grant No. 511-1009406). The beamline time of Shanghai Synchrotron Radiation Facility (SSRF) is also gratefully acknowledged.

Supplementary data to this article can be found online at http://dx.doi.org/10.1016/j.scriptamat.2017.03.030.

References

[1] P.J. Withers, M. Preuss, Annu. Rev. Mater. Res. 42 (2012) 81.
[2] T. Zhang, J. Jiang, B. Britton, B. Shollock, F. Dunne, Proc. R. Soc. A 472 (2016) 20150792.
[3] K. Lu, Science 345 (2014) 1455.
[4] X. Wu, M. Yang, F. Yuan, G. Wu, Y. Wei, X. Huang, Y. Zhu, Proc. Natl. Acad. Sci. U. S. A. 112 (2015) 14501.
[5] M. Koyama, Z. Zhang, M. Wang, D. Ponge, D. Raabe, K. Tsuzaki, H. Noguchi, C.C. Tasan, Science 355 (2017) 1055.
[6] X. Ma, C. Huang, J. Moering, M. Ruppert, H.W. Höppel, M. Göken, J. Narayan, Y. Zhu, Acta Mater. 116 (2016) 43.
[7] H. Wu, B.C. Jin, L. Geng, G. Fan, X. Cui, M. Huang, R.M. Hicks, S. Nutt, Metall. Mater. Trans. A 46 (2015) 3803.
[8] M.Y. Seok, J.A. Lee, D.H. Lee, U. Ramamurty, S. Nambu, T. Koseki, J.I. Jang, Acta Mater. 121 (2016) 164.
[9] J. Wang, Q. Zhou, S. Shao, A. Misra, Mater. Res. Lett. 5 (2017) 1.
[10] M. Huang, G.H. Fan, L. Geng, G.J. Cao, Y. Du, H. Wu, T.T. Zhang, H.J. Kang, T.M. Wang, G.H. Du, H.L. Xie, Sci. Rep. 6 (2016) 38461.
[11] T.H. Fang, W.L. Li, N.R. Tao, K. Lu, Science 331 (2011) 1587.

[12] X.L. Wu, M.X. Yang, F.P. Yuan, L. Chen, Y.T. Zhu, Acta Mater. 112 (2016) 337.
[13] H.L. Xie, B. Deng, G.H. Du, Y.N. Fu, R.C. Chen, G.Z. Zhou, Y.Q. Ren, Y.D. Wang, Y.L. Xue, G.Y. Peng, Y. He, H. Guo, T.Q. Xiao, Nucl. Sci. Tech. 26 (2015) 020102.
[14] R.J. Arsenault, N. Shi, C.R. Feng, L. Wang, Mater. Sci. Eng. A 131 (1991) 55.
[15] H. Wu, G. Fan, M. Huang, L. Geng, X. Cui, H. Xie, Int. J. Plast. 89 (2017) 96.
[16] H.J. Gao, B.H. Ji, I.L. Jäger, E. Arzt, P. Fratzl, Proc. Natl. Acad. Sci. U. S. A. 100 (2003) 5597.
[17] S.D. Antolovich, R.W. Armstrong, Prog. Mater. Sci. 59 (2014) 1.
[18] J. Li, G.J. Weng, S. Chen, X. Wu, Int. J. Plast. 88 (2017) 89.
[19] W. Guo, E. Jägle, J. Yao, V. Maier, S. Korte-Kerzel, J.M. Schneider, D. Raabe, Acta Mater. 80 (2014) 94.
[20] X.L. Ma, C.X. Huang, W.Z. Xu, H. Zhou, X.L. Wu, Y.T. Zhu, Scr. Mater. 103 (2015) 57.